Electromechanical Energy Conversion Systems (EECS),
Niroo Research Institute.
Vol. 1, Issue. 2 . Spring 2021

Research on Effective Parameters on Overvoltage and Inrush Current During Starting-up of VSC-HVDC System

Mahmudreza Changizian[1], Abbas Shoulaie[2*]

[1]Department of Electrical Engineering, Iran University of Science and Technology
Tehran, Iran

**Corresponding author, Email: [1]m_changizian@elec.iust.ac.ir, [2]shoulaie@iust.ac.ir*

Abstract

The starting-up strategy is an important issue for voltage source convert-high voltage direct current (VSC-HVDC) system. If a VSC-HVDC system starts up without any auxiliary system or improved control system, overvoltage and inrush current will occur. This large overvoltage can cause serious damage on the DC capacitors and this large inrush current at turn-on may destroy the switches in converter. Starting-up VSC-HVDC has two steps. In this paper, starting-up steps in a three-phase two-level VSC-HVDC system is studied with details. The effect of capacitor and inductor sizes and also circuit breaker closing time on overvoltage and inrush current in first step are investigated attentively. Possible methods for control overvoltage and inrush currents during this step are presented, and a comparison has been made between them in terms of power dissipation and cost. Eventually, the best auxiliary starting-up system is selected in terms of costs. In addition, the second step of starting-up is also examined and the circuit performance for increasing the DC link voltage is described in this step. Also, a simple control method is proposed for controlling the inrush current in second step. This method controls the inrush current without imposing additional costs and losses on the system. Substantial simulations conducted on PSCAD/EMTDC platform. It is worth mentioning this paper is an extended version of the paper accepted at the 34th Power System Conference (PSC 2019).

Keywords: VSC-HVDC; Starting-up; Inrush current; Overvoltage; Diode bridge rectifier; PWM-Rctifier

1. INTRODUCTION

Since the so-called "war of currents" that took place in New York in the 19th century between DC and AC systems, AC system has been the main platform for power transmission. Although AC power was perfectly adequate for the conditions of the day and met most of the needs of the 20th century, but against the needs of the 21st century are showing its limits. The truth is, although DC system lost the battle, it is making a comeback by High Voltage Direct Current (HVDC) technology[1]. The advantages of HVDC transmission over HVAC include: low voltage drop, low insulation level, less power losses, greater maximum distance and transmission power, more reliability, optimal use of power plants, lower cost over long distances, and ability to connect asynchronous grids [2, 3]. General HVDC applications include the following: very long transmission lines, asynchronous interconnection, cable transmission lines, bulk power delivery, and submarine cable crossings [4-6].

In a general classification, converters used in HVDC structures can be divided into two types of line-commutated current-source converter (LCC or CSC) and forced commutated voltage source converter (VSC) [7]. The CSC-HVDC technology is built using thyristor bridges and works on line commutation. For this reason, all terminals require the existence of an AC generator with rotating machines and high short-circuit ratio. CSC-HVDC structure will always be reactive power consumption. As a result, it is not possible to independently control active and reactive power in this structure [8]. Forced-commutated VSCs are use PWM bridges with gate turn-off thyristors (GTOs) or insulated gate bipolar transistors (IGBTs) in most industrial cases. This technology can be easily used in passive or weak grids. In this system, it is possible to

independently control active and reactive power [7]. A brief summary of the differences between VSC and CSC technology is presented in TABLE I [8]. VSC-HVDC structure, due to the additional advantages, finds other applications that have been addressed in various literature [9-13].

To operate VSC-HVDC, the system must start-up at first. During starting-up VSC-HVDC, DC-side capacitors are in discharge mode, so diodes are forward biased and IGBTs are blocked. Therefore the VSC acts as a diode rectifier and charges the capacitors. For a VSC-HVDC system, the equivalent resistance, which mainly consists of the commutation resistance and the equivalent resistance of converter station, is quiet small. At the first moment, discharged capacitors act as a short circuit and cause inrush current during start-up. This overvoltage can damage the capacitors. In addition, large currents at start-up may cause harm to switches[14, 15]. Two practical projects, Cross sound cable project [16] and Murrylink project [17], first report that the switch tubes in the valve are burned down because of overcurrent, and the differential under voltage protection is mis-operated in the procedure of starting-up[14]. Therefore, starting-up is one of the challenges of VSC-HVDC structure and different methods are presented to solve this problem in literature [18-23].

TABLE 1. COMPARISON BETWEEN VSC-HVDC AND CSC-HVDC

Technology	CSC-HVDC	VSC-HVDC
Semiconductor	Thyristor	IGBT
Power Control	Active	Active/Reacitve
AC Filters dimension	Large	Small
Minimum Short Circuit Ratio	>2	0
Black Start Capability	No	Yes

The rest of this paper is organized as follows: performances of a three-phase two-level VSC-HVDC system without auxiliary starting-up strategy and impact of various factors (DC capacitors, phase reactor, and closing time of AC circuit breakers) on overvoltage and inrush current are analysis in Section II. In Section III, possible methods for control of overvoltage and inrush current during starting-up are presented and a comparison in terms of power dissipation and costs is done between them and finally the best method is chosen. In Section IV, a new DC voltage control method is proposed to limit inrush current during start up. Simulation results based on the selected starting-up strategy are given in Section V, which shows that the selected strategy can restrain the overcurrent effectively. Section VI recaps the main conclusions of this paper. This paper is an extended version of the paper accepted at the 34th Power System Conference (PSC 2019) [24].

2. Starting-up VSC-HVDC system

A. Typical structure and control principle

A two-level VSC is one of the typical structure in VSC-HVDC system. In this paper, the research is based on a two-level VSC-HVDC system, which consists of AC grid, converter transformer, AC filter, AC breaker (S1), phase reactor (L), DC capacitors (C), and a converter bridge, as shown in Fig. 1. This system is considered as an ideal system and phase resistance is assumed to be zero. According to Fig. 1 the active and reactive power exchange (P and Q) as seen from the AC system terminals can be expressed respectively as:

$$S = U_s\angle 0\left(\frac{U_s\angle 0 - U_C\angle\delta}{X\angle\frac{\pi}{2}}\right) \quad (1)$$

$$P = \frac{U_s U_c}{X} sin\ \delta \quad (2)$$

Figure 1. Two-level topology structure of VSC-HVDC system

$$Q = -\frac{U_s(U_s - U_c cos\delta)}{X} \quad (3)$$

where X is the phase reactance with X = ωL; ω is the angular frequency of AC grid with ω = 2π f. According to this equation, δ and U_c play an important role in determining the magnitudes of active and reactive powers, which are the main control variables. U_c is as follow:

$$U_c = \frac{M}{\sqrt{2}} \times U_{dc} \quad (4)$$

Where M is the modulation index. Therefore the amount of absorbed active and reactive power by the VSC are depended on the phase index (δ) and the modulation index (M) of the VSC converter.

B. Steps of starting-up in VSC-HVDC

The VSC-HVDC system start up consists of two stages: (i) Uncontrolled rectifier stage, charge DC capacitors up to the maximum of the AC line voltage (ii) Controlled voltage stage, boosting the capacitor voltage from the line voltage up to the desirable DC voltage. When circuit breaker (CB) is closed IGBTs are blocked and all diodes are connected AC side to DC side. System operate as a three-phase uncontrolled rectification circuit. Thus, this period is called uncontrolled rectifier stage. In this stage, AC power

grid pre-charges DC capacitors [16]. In second stage IGBTs are deblocked and fixed DC voltage controller starts working in this moment, DC voltage can be controlled. Therefore, this period is called controlled voltage stage. In order to reduce DC transmission line losses and to have control on turn-on and turn-off of switches, usually DC link voltage in VSC-HVDC system will be exceeded than AC voltage in this stage.

C. Inrush current and overvoltage in Uncontrolled rectifier stage without auxiliary starting-up system

In VSCs during start-up, considerable overvoltage and large inrush currents can result if the AC voltage is suddenly applied to the circuit by means of a contractor. As mentioned in previous section, parallel diodes with IGBTs operate as a diode rectifier at first moments, and due to capacitor is initially completely discharged, a large inrush current is drained from grid to charge capacitor. The theoretical maximum voltage across the capacitor due to this series L-C connection approaches $2\sqrt{2}V_s$ for certain L and C.

This large overvoltage can cause serious damage on the DC capacitors and this large inrush current at turn-on may destroy switches in the converter.

Fig. 2 shows the three-phase diode bridge rectifier that created during the start-up of the VSC-HVDC system. Therefore, it can be concluded, value of capacitors (C), value of inductors (L) and CB closing time are affecting the amount of overvoltage and inrush currents that will be studied in the following.

1) Impact of capacitor and inductor values on overvoltage and inrush current

It is assumed that CB1 is closed at t=0s. Therefore, due to the short circuit at the dc side and according to the currents directions ($i_a > 0, i_b < 0, and\ i_c > 0$) at the ac side, D1, D5, and D6 will be turned-on. After closing CB1 and at the initial moment, currents path and charging capacitor path are shown in Fig. 3 with red dashed lines. Thus, in this mode the current and voltage equations are as follows:

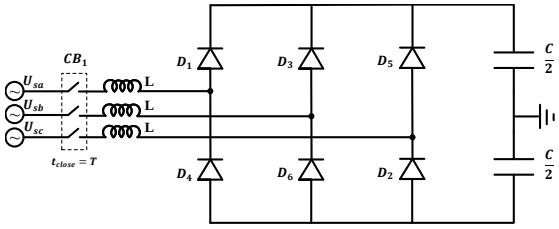

Figure 2. Equivalent circuit of uncontrolled rectifier stage without auxiliary starting-up system

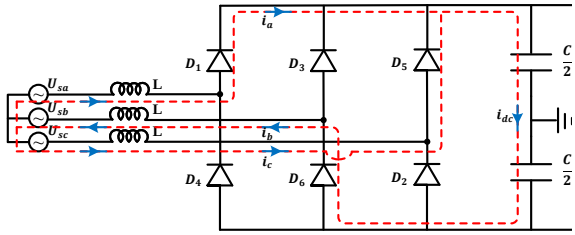

Figure 3. Currents path and charging capacitor path at the initial moment

$$\begin{cases} U_{sa} = V_m \sin(\omega t) \\ U_{sb} = V_m \sin(\omega t - 120) \\ U_{sc} = V_m \sin(\omega t + 120) \end{cases} \tag{5}$$

$$L\frac{d^2 i_a}{dt^2} + L\frac{d^2 i_b}{dt^2} + \frac{1}{C} i_b = \frac{dU_{sab}}{dt} \tag{6}$$

$$L\frac{di_a}{dt} - L\frac{di_c}{dt} = -U_{sca} \tag{7}$$

$$i_c = i_b - i_a \tag{8}$$

Therefore

$$L\frac{di_b}{dt} - 2L\frac{di_a}{dt} = U_{sca} \tag{9}$$

$$\frac{3L}{2}\frac{d^2 i_b}{dt^2} + \frac{1}{C} i_b = \frac{1}{2}\frac{dU_{sca}}{dt} + \frac{dU_{sab}}{dt} \tag{10}$$

Where i_a, i_b, and i_c are the phase currents, U_{sab} is the line voltage between phase a and phase b, U_{sca} is the line voltage between phase c and phase a. Equation of DC link voltage is as follows:

$$U_{dc} = \frac{1}{C}\int i_b dt + U_{dc0} \tag{11}$$

By solving the second-order equations, the capacitor voltage and phase currents equations are obtained based on L and C parameters. According to the obtained equations at start-up moment, effect of capacitor and inductor changes on maximum of overvoltage and inrush current is shown in fig. 4 to fig.7. In this study, U_{s-rms} is 24.5 kV and f is 50Hz.

Inrush current usually has very little energy but has devastating effects. As it can be seen in Fig. 4, by increasing the capacitor value based on $\frac{1}{2}CV^2$ equation,

inrush current is not able to raise the DC voltage very much and as a result the

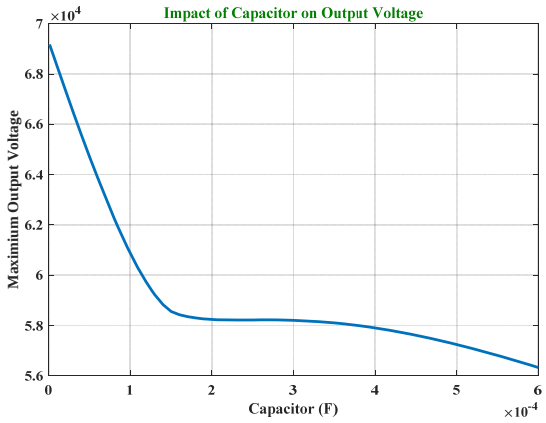

Figure 4. Overvoltage at start-up moment based on capacitor value (L = 4.8mH)

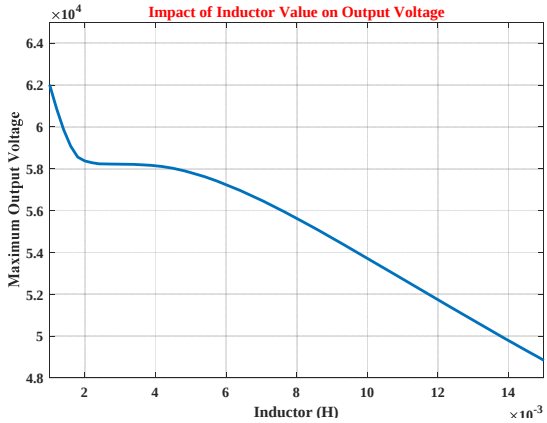

Figure 5. Overvoltage at start-up moment based on inductor value ($C = 400\mu F$)

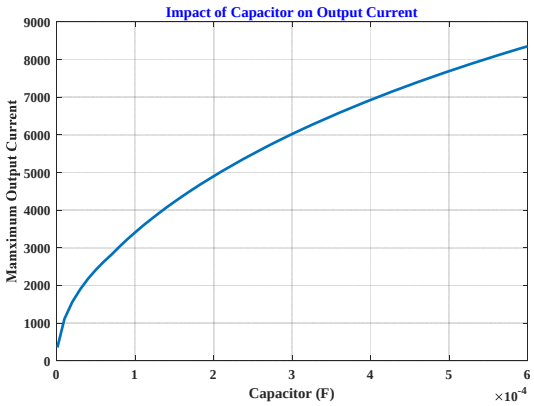

Figure 6. Inrush current at start-up moment based on capacitor value (L = 4.8mH)

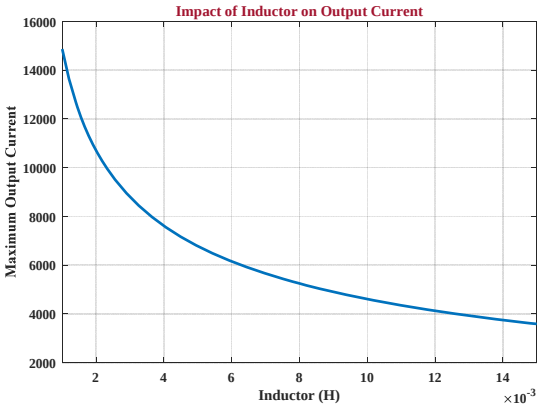

Figure 7. Inrush current at start-up moment based on inductor value ($C = 400\mu F$)

overvoltage decreases. As the capacitor value increases, effect of the inductor gradually decreases and the circuit becomes like a junction of two voltage sources, which causes the impulse current in theory. Therefore, the inrush current increases by increasing capacitor value, that this outcome is shown in Fig. 6. The effect of increasing inductor value on the inrush current is shown in Fig. 7 that cause to reduce inrush current, and also reduce overvoltage due to growing up of inertia (see Fig. 5). Also in Fig. 8 and Fig. 9 simultaneous effect of changes in inductor and capacitor values on the amount of overvoltage and inrush current are shown in the three-dimensional (3D) curves. Therefore, in design of L and C, overvoltage and inrush current can be considered as determining parameters in addition to other parameters and make an optimal design for capacitor and inductor based on them.

2) Impact of CBs closing time on overvoltage and inrush current

Fig. 10 shows the effect of CB closing time on the overvoltage and inrush current. The closing time of CB varies from zero to 90 degree. As can be seen from Fig. 10, the closing time of CB is effective on overvoltage and inrush current, but it has very little affect compared to capacitor and inductor values.

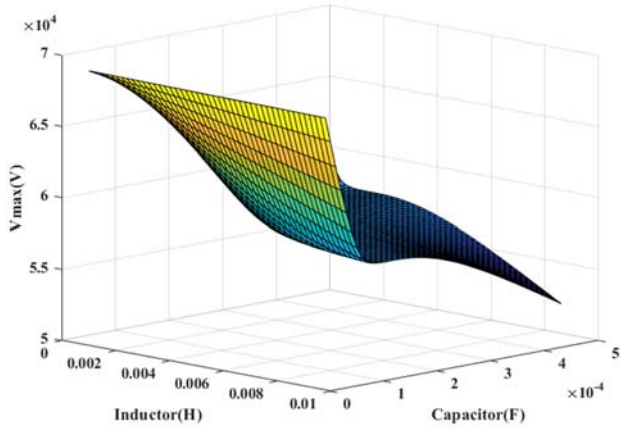

Figure 8. Simultaneous effect of change in capacitor and inductor values on start-up overvoltage

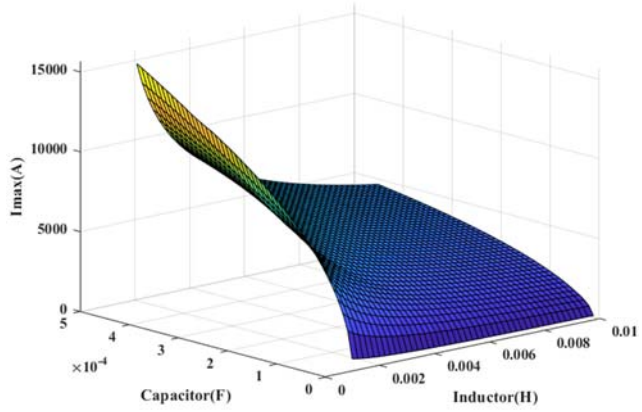

Figure 9. Simultaneous effect of change in capacitor and inductor values on start-up inrush current

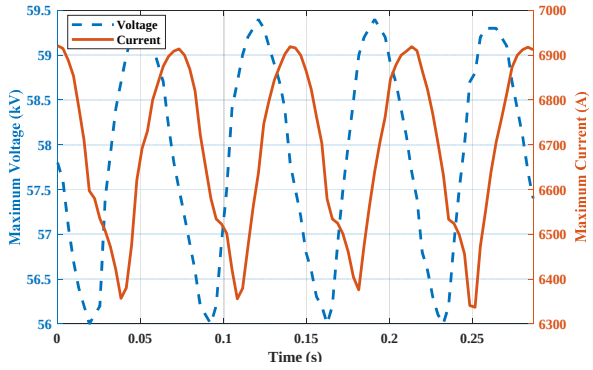

Figure 10. Impact of CBs closing time on overvoltage and inrush current ($C = 400\mu F, L = 4.8mH$)

D. Inrush current in Controlled voltage stage during starting-up

After charging the capacitors to the maximum line voltage, the second stage of starting-up process is starting. In second stage of starting-up, the DC link voltage should be charged as much as the reference voltage, which is usually greater than the maximum line voltage. This is done for two reasons: 1) Reduce DC line power loss and 2) To have control on turn-on and turn-off of switches (IGBTs controllability). If the DC line voltage charging up to the maximum line voltage, when the capacitor voltage drops because of the power flow, the control process get into trouble due to unwanted diodes conduction (IGBTs controllability disappears) [25]. Therefore, in the second stage the VSC converter acts as a PWM-rectifier and increases the DC link voltage. At this stage, upper or lower switches must be turned on at first to current flow in inductors by shortening them, and then by sequential switching, the inductors' energy is transferred to the capacitors, which increases the capacitor voltage according to the capacitor energy equation. The IGBT or diode conductivity of each switch depends on the direction of current flowing in the inductors at the instant of the shortening. But when transmitting energy to capacitors only diodes are on(such as diode rectifier mode). Depending on the possible modes for currents way there are six different modes that are shown in Table II. The equivalent circuit of this process for the special case ($i_a > 0, i_b > 0 \; and \; i_c < 0$) is shown in Fig. 11.

As is clear in the Fig. 11, three lower switches are given a pulse at first to shorten the inductors and current flow. IGBT4, IGBT6 and D2 are on depends on current direction. At this stage the capacitor current is zero and the capacitor voltage remains constant. In the next step, all pulses must be cut of then the current of the inductor pass through the capacitor (from D1, D3 and D2 like Fig. 12) and increase its voltage. This process continues with the PWM switching method. If the PWM rectifier is controlled by the PI controller, it wants to supply DC link voltage very quickly to the reference value, thus causing a severe inrush current which can damage the switches and even burn them. This inrush current can be more intense than the first stage of start-up. Some methods are proposed to prevent inrush current at this stage [14]. Increasing the equivalent resistance results in the cost of losses and additional equipment to the system and in addition increases the time to reach the reference voltage. So the desirable method is that, get the voltage to the reference value without imposing additional cost on the system. In this paper, a simple control method is proposed to reduce and control the inrush current in second stage of starting-up.

3. Possible methods for control overvoltage and inrush currents in Uncontrolled rectifier stage

In [14, 20-23, 26, 27] used resistors for a few cycles on the AC side to limit the inrush current. In [15] suggested to put resistor between capacitor and rectifier to limit the inrush current in diode rectifiers. In [25] uses the DC voltage regulator to charge capacitor slowly in the laboratory sample.

TABLE 2. SIX DIFFERENT MODES FOR CURRENTS WAY

Phase Current	i_a	i_b	i_c
Two positive phase current	+	+	-
	+	-	+
	-	+	+
Two negative phase current	-	-	+
	-	+	-
	+	-	-

In [28] recommends replacing diodes with IGBT to control the current at any desired value. Replacing diodes with IGBT greatly increases the system cost and makes it more complex to control, also variable DC voltage sources from the aspect of operating and availability has some problems. Considering the previous section, in addition to these methods, the use of inductors on the DC side or on the AC side can also have a large impact on the start-up inrush current, but due to the high cost and complexity of design, this method may not be very attractive. Therefore, in terms of cost and ease of implementation the use of resistor on AC and DC sides is justified. These two methods will be compared in terms of cost and power dissipation in the following.

E. Use of three resistors and three CBs on the AC side

Equivalent circuit of uncontrolled rectifier stage with three resistors and three CBs is shown in Fig. 13. At start-up, circuit breaker S_1 are closed and resistors are placed in the circuit to limit current and voltage. After a few cycles, circuit breaker S_2

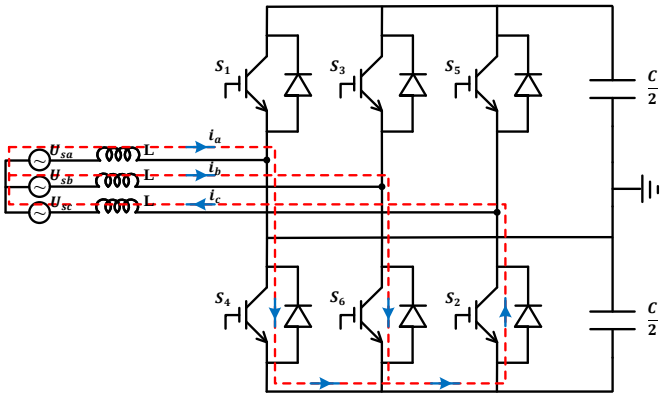

Figure 11. Lower switches are are given a pulse and current flow in inductors from IGBT4, IGBT6 and D2 ($i_a > 0, i_b > 0$ *and* $i_c < 0$)

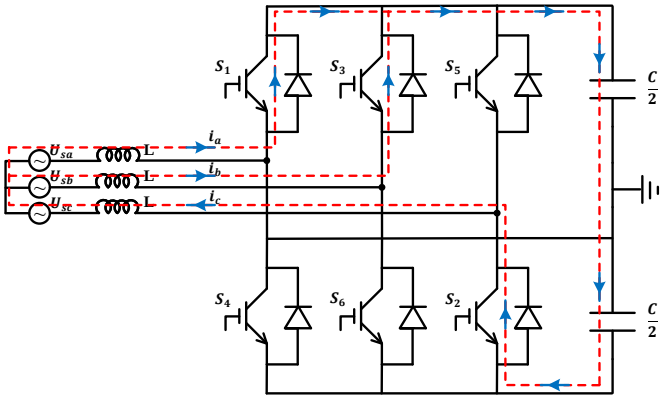

Figure 12. Current of the inductor pass through the capacitor from D1, D3 and D2 (Charging path)

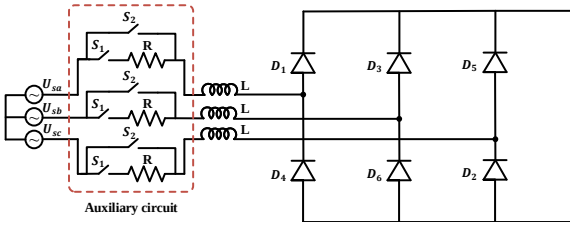

Figure 13. *Starting-up diagram* with three resistors and three CBs

are closed and resistors (R) are bypassed. In this circuit, current and voltage equations at start-up time are as follows:

$$L\frac{d^2 i_a}{dt^2} + L\frac{d^2 i_b}{dt^2} + R\frac{di_a}{dt} + R\frac{di_b}{dt} + \frac{1}{C}i_b = \frac{dU_{sab}}{dt} \qquad (12)$$

$$L\frac{di_a}{dt} - L\frac{di_c}{dt} + Ri_a - Ri_c = -U_{sca} \quad (13)$$

$$i_c = i_b - i_a \quad (14)$$

Therefore

$$L\frac{di_b}{dt} + Ri_b - 2L\frac{di_a}{dt} - 2Ri_a = U_{sca} \quad (15)$$

$$\frac{3L}{2}\frac{d^2i_b}{dt^2} + \frac{3R}{2}\frac{di_b}{dt} + \frac{1}{C}i_b = \frac{1}{2}\frac{dU_{sca}}{dt} + \frac{dU_{sab}}{dt} \quad (16)$$

$$U_{dc} = \frac{1}{C}\int i_b dt + U_{dc0} \quad (17)$$

Considering the initial conditions and solving the second-order equations, the capacitor voltage and phase currents equations are obtained based on R, L, and C parameters. Fig. 14 shows the maximum voltage and current curves based on resistor size (R) during start-up and as expected before, the amount of overvoltage and inrush current decreases as resistance increased. In Fig. 15, the maximum power loss and the maximum voltage on the CBs (S_2) can be seen based on resistor size (R). By increasing resistor size, the maximum power loss decreases and the maximum voltage on CBs increases, therefore the cost related to resistor and power loss decrease but CBs size and its cost increase. In this study $U_s = 24.5kV, L = 4.8mH, and\ C = 400\mu F$.

F. Use of one resistor and one switch on the DC side

The equivalent circuit at start-up is shown in Fig. 16. In this case, unlike the previous circuit, short circuit is not happened at DC side due to presence R_{dc}. Therefore, at start-up only two diodes (if S_1 is closed at t = 0s) D5 and D4 conduct and the current path is marked with a red dashed line in Fig. 16. At start-up, circuit breaker S_1 are closed and R_{dc} are placed in the circuit to limit current and voltage. After a few cycles, switch S_2 are closed and resistors is bypassed. In this circuit, current and voltage equations at start-up time are as follows:

$$L\frac{di_c}{dt} + R_{dc}i_c + V_{cap} + L\frac{di_b}{dt} = -U_{sbc} \quad (18)$$

$$i_c = i_b \quad (19)$$

Therefore

$$2L\frac{di_b}{dt} + R_{dc}i_b + V_{cap} = -U_{sbc} \quad (20)$$

$$2L\frac{d^2i_b}{dt^2} + R_{dc}\frac{di_b}{dt} + \frac{1}{C}i_b = -\frac{dU_{sbc}}{dt} \quad (21)$$

$$U_{dc} = \frac{1}{C}\int i_b dt + U_{dc0} \quad (22)$$

This resistor shorted out, either by a mechanical contactor or by a thyristor after a few cycles subsequent to turn-on [15]. Fig. 17 shows the maximum voltage and current curves based on resistor (R_{dc}) during start-up and as expected before, the amount of overvoltage and inrush current decreases as resistance increased.

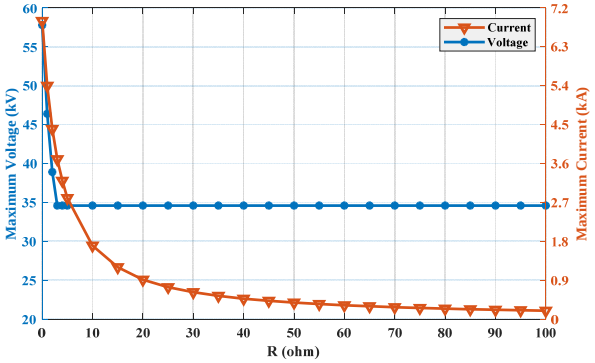

Figure 14. Maximum voltage and current based on resistor (R) during start-up

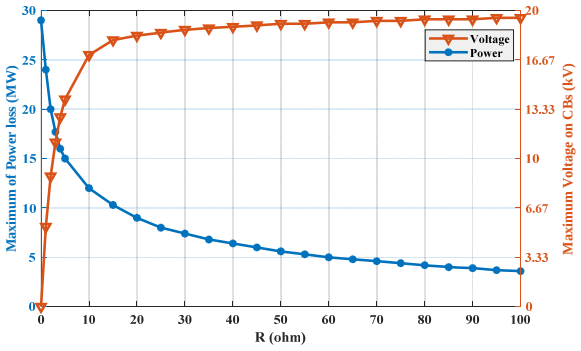

Figure 15. Maximum of power loss and voltage on the CBs (S2) based on resistor (R) during start-up

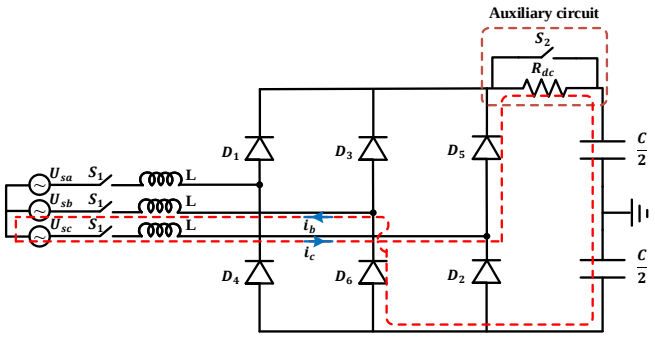

Figure 16. *Starting-up diagram* with one resistor and one switch at DC side

In Fig. 17, the maximum power loss and the maximum voltage on S_2 can be seen based on resistor size (R_{dc}). By increasing resistor size, the maximum power loss decreases and the maximum voltage on S_2 increases, therefore the cost related to resistor and power loss decrease but size of S_2 and its cost increase. In this study $U_s = 24.5kV, L = 4.8mH, and\ C = 400\mu F$.

G. Choosing suitable start-up method from power loss and cost perspective

Among the possible methods for start-up VSC-HVDC system, using resistor at DC and AC side were selected from the cost perspective. The performance of the system at start-up was analyzed when using these two methods. Regarding the equations and curves from the power loss perspective, these two methods are not much different. But the voltage on S_2 at DC side is approximately 1.7 times the voltage on S_2 at AC side. It should be noted that in VSC-HVDC system, due to the increasing DC voltage in normal operating mode, DC side current will be lower than AC side current. Therefore, it can be concluded, the cost of three switches at AC side will be higher than one switch at DC side. As an result, using one resistor and one switch at DC side is cost efficient and more appropriate for auxiliary starting-up system in VSC-HVDC.

4. Proposed method to reduce inrush current in Controlled voltage stage during starting-up

The control system of VSC-HVDC is consist of two section, outer controller and inner current controller. Vector control system diagram of VSC-HVDC is shown in Fig. 19. $I_{dref}, I_{qref}, U_{Cdref}$ and U_{Cqref} are the reference current and voltage respectively in dq0 reference frame. Outer controller should control two parameter in each terminal. In one station, DC voltage must be controlled for stablish power balance between the AC and DC side. Another controlled parameter will be selected between AC voltage and reactive power to control in this terminal. In second stage of starting-up the control system will be active and fixed DC voltage controller starts working in this moment. In conventional methods the reference voltage signal (U_{DCref}) is changed as a step function to growth the DC link voltage to the desired value as shown in

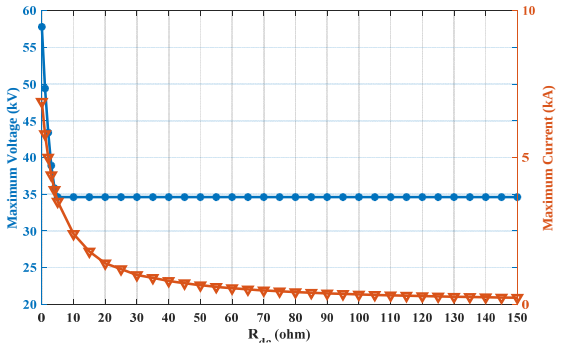

Figure 17. Maximum voltage and current curves based on resistor size (R_{dc}) during start-up

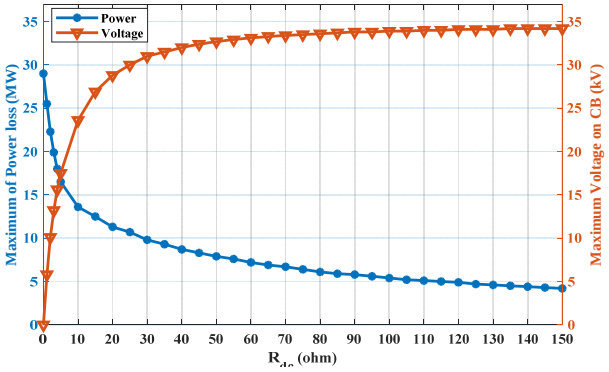

Figure 18. Maximum power loss and maximum voltage on switch (S2) based on resistor size (R_{dc}) during start-up

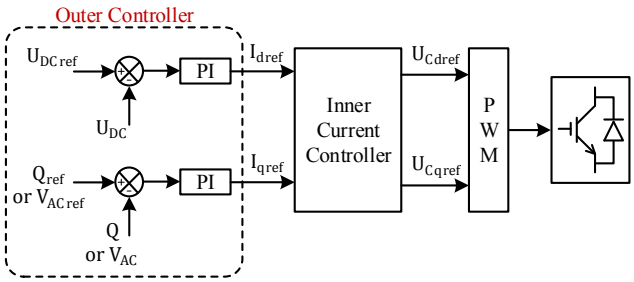

Figure 19. The control diagram of VSC-HVDC

Fig. 20. This kind of sudden change in the reference voltage is an important factor in generating inrush current. Therefore, if the reference voltage signal that is impose to control system is increased slowly and reaches to the desired value by specified change in several steps, the inrush current decreases and even its

value can be controlled. The proposed method for changing reference voltage in this paper is shown in Fig. 21. In this method, U_{DCref} is changed with a gentle slope in several steps. The magnitude of the change of each step will affect the amplitude of current.

5. Simulation Verification

To ensure the good starting-up characteristics of VSC-HVDC with R_{dc} at DC side, a two-level VSC-HVDC system (Fig. 1) is built in PSCAD/EMTDC platform. The relevant parameters of the system are given in Table II. The overcurrent allowable value is determined by the rated current of the system and its switches. So overcurrent allowed by VSC-HVDC system (i_{max}) is 1.54 kA (1.1pu). The overvoltage of AC side allowed by VSC- HVDC system (U_{max}) is 57.5 kV (1.15 pu). R_{dc} is determined first (based on equation 21 and i_{max} condition). Therefore, the obtained value for R_{dc} is 21 Ω. The starting-up process can be expressed as follows:

i) At 0□<□t□<□0.1 (s), S_1 is switched off. The whole system is shutdown state.

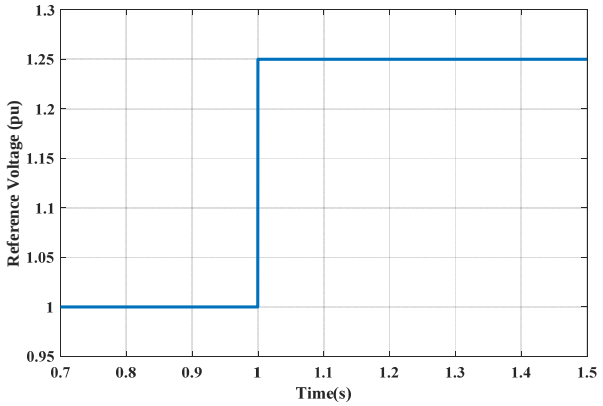

Figure 20. Conventional function for reference voltage signal

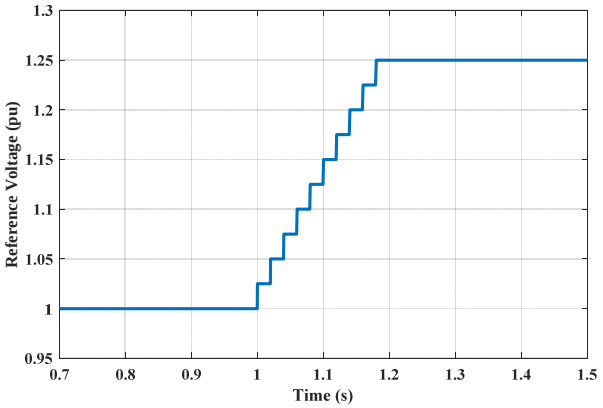

Figure 21. Proposed function for reference voltage signal

ii) At t□=□0.1 (s), S_1 is switched on. IGBTs are blocked. All diodes are connected AC side to DC side. They consist of a three-phase uncontrolled rectification circuit, as shown in Fig. 2.

iii) At t□=□0.5 (s), S_2 is switched on. R_{dc} shorted out.

iv) At t□=□1 (s), IGBTs are deblocked. Fixed DC voltage controller starts working. From this moment, DC voltage can be controlled.

v) t□=□1.5 (s), active power controller starts working.

vi) At t□=□2 (s), reactive power controller starts working.

The simulation results are shown in Fig. 22, Fig. 23 and Fig. 24. The results show auxiliary system is operating properly as expected. But as shown in the Fig. 22, the inrush current in the second stage is more than the allowable current. Now the simulation is repeated with proposed control method and its results are shown in Fig. 24. As is clear, in second stage with proposed method the DC link voltage increases with slow slope based on reference function and inrush current decreases without any extra equipment or cost. In this case, inrush current is reduced 0.65kA in the second stage and becomes lower than the maximum permitted value.

6. Cunclusion

In this paper, starting-up steps and its details were analyzed in a three-phase two-level VSC-HVDC system. Effect of DC capacitor and inductor sizes and CBs closing time, on overvoltage and inrush current in first step of starting-up were investigated. It was shown, inductor and capacitor sizes will have a large effect on overvoltage and inrush current, so these parameters can be considered in design of L and C and choose optimal value for them. All possible methods for controlling VSC-HVDC system during first step of starting-up have been presented and a comparison has been made between them in terms of power dissipation and costs. Eventually, one resistor and one switch on the DC side was selected that is the best auxiliary starting-up system in terms of costs. The second step of starting-up was examined and a simple control method was proposed for controlling the inrush current in this step. This proposed method, controls the inrush current without imposing additional costs and losses to the system. The presented simulation results show that the proposed strategy can restrain the overcurrent effectively.

TABLE 3. OPERATING PARAMETERS

Parameter	Rated Value
Phase reactance	4.8 mH
DC capacitor	400 μF
Transformer ratio	110/24.5 kV
Line-Line AC voltage (VLL)	24.5 kVrms
DC voltage	50 kV
Rated power	70 MVA
Reference active power	50MW
Reference reactive power	30MW

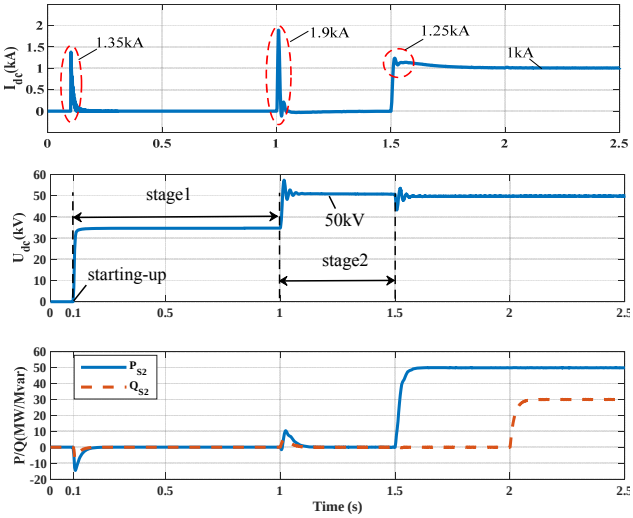

Figure 22. Simulation results of VSC-HVDC system with auxiliary starting-up system at DC side

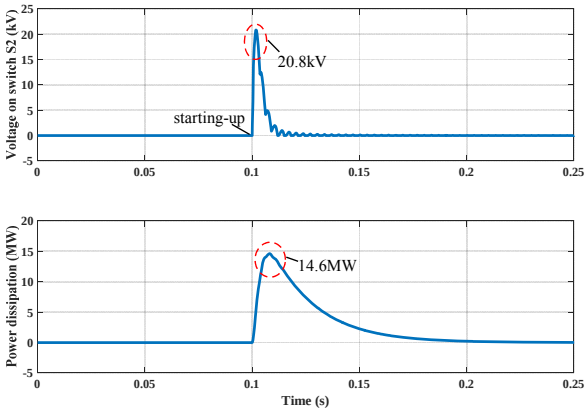

Figure 23. Power dissipation and blocking voltage S2 during starting-up process

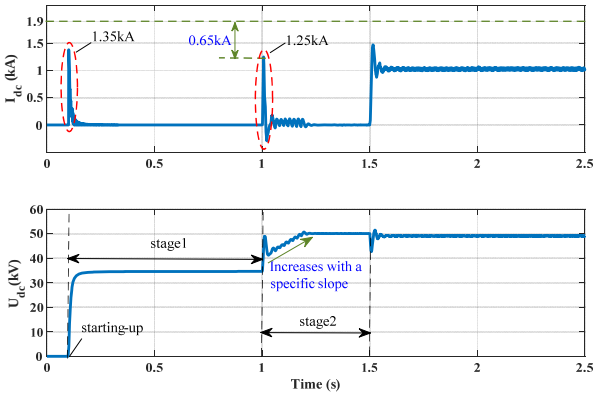

Figure 24. Simulation results of VSC-HVDC system with proposed control method

7. References

[1] N. Stenberg, "The impact of HVDC innovations on the power industry," Master of Science, Industrial Economics and Management, KTH Industrial Engineering and Management, 2013.

[2] K. R. Padiyar, *HVDC power transmission systems: technology and system interactions*. New Age International, 2010.

[3] M. Eremia, C.-C. Liu, and A.-A. Edris, *Advanced solutions in power systems: HVDC, FACTS, and Artificial Intelligence*. John Wiley & Sons, 2016.

[4] J. Lin, "Integrating the First HVDC-Based Offshore Wind Power into PJM System—A Real Project Case Study," *IEEE Transactions on Industry Applications*, vol. 52, no. 3, pp. 1970-1978, 2016, doi: 10.1109/TIA.2015.2511163.

[5] Z. Xu, S. Wang, and H. Xiao, "Hybrid high-voltage direct current topology with line commutated converter and modular multilevel converter in series

connection suitable for bulk power overhead line transmission," *IET Power Electronics,* vol. 9, no. 12, pp. 2307-2317, 2016, doi: 10.1049/iet-pel.2015.0738.

[6] W. Xiang, R. Yang, C. Lin, J. Zhou, J. Wen, and W. Lin, "A Cascaded Converter Interfacing Long Distance HVDC and Back-to-Back HVDC Systems," *IEEE Journal of Emerging and Selected Topics in Power Electronics,* pp. 1-1, 2019, doi: 10.1109/JESTPE.2019.2913915.

[7] N. Flourentzou, V. G. Agelidis, and G. D. Demetriades, "VSC-based HVDC power transmission systems: An overview," *IEEE Transactions on power electronics,* vol. 24, no. 3, pp. 592-602, 2009.

[8] R. Sellick and M. Åkerberg, "Comparison of HVDC Light (VSC) and HVDC Classic (LCC) site aspects, for a 500MW 400kV HVDC transmission scheme," 2012.

[9] P. Bresesti, W. L. Kling, R. L. Hendriks, and R. Vailati, "HVDC connection of offshore wind farms to the transmission system," *IEEE Transactions on energy conversion,* vol. 22, no. 1, pp. 37-43, 2007.

[10] B. Westman, S. Gilje, and M. Hyttinen, "Valhall re-development project, power from shore," in *PCIC Europe 2010*, 2010: IEEE, pp. 1-5.

[11] C. Du, M. H. Bollen, E. Agneholm, and A. J. I. T. o. P. D. Sannino, "A new control strategy of a VSC–HVDC system for high-quality supply of industrial plants," vol. 22, no. 4, pp. 2386-2394, 2007.

[12] R. Yang, G. Shi, X. Cai, C. Zhang, G. Li, and J. Liang, "Autonomous Synchronizing and Frequency Response Control of Multi-terminal DC Systems with Wind Farm Integration," *IEEE Transactions on Sustainable Energy,* pp. 1-1, 2020, doi: 10.1109/TSTE.2020.2964145.

[13] C. M. Diez, A. Costabeber, F. Tardelli, D. Trainer, and J. Clare, "Control and Experimental Validation of the Series Bridge Modular Multilevel Converter for HVDC Applications," *IEEE Transactions on Power Electronics,* vol. 35, no. 3, pp. 2389-2401, 2020, doi: 10.1109/TPEL.2019.2929862.

[14] S. Lin, L. Wang, D. Mu, L. Liu, K. Liao, and Z. J. I. R. P. G. He, "Research on starting-up control strategy of VSC-HVDC system," vol. 12, no. 16, pp. 1957-1965, 2018.

[15] N. Mohan, T. M. Undeland, and W. P. Robbins, *Power electronics: converters, applications, and design*. John wiley & sons, 2003.

[16] I. Mattsson *et al.*, "Murraylink, the longest underground HVDC cable in the world," in *Paper B4-103 presented at the Cigré conference, Paris, France, Aug*, 2004.

[17] L. Ronström *et al.*, "Cross sound cable project second generation VSC technology for HVDC," in *Cigré Session*, 2004, pp. B4-102.

[18] C. Zhao and Y. Sun, "Study on control strategies to improve the stability of multi-infeed HVDC systems applying VSC-HVDC," in *2006 Canadian Conference on Electrical and Computer Engineering*, 2006: IEEE, pp. 2253-2257.

[19] H.-r. CHEN, J. Zhang, and W.-l. PAN, "Start-up Control of VSC Based on HVDC System [J]," *High Voltage Engineering,* vol. 5, pp. 1164-1169, 2009.

[20] S. K. Chaudhary, "Control and protection of wind power plants with VSC-HVDC connection," *Aalborg University, Aalborg,* 2011.

[21] S. K. Chaudhary, R. Teodorescu, P. Rodriguez, P. Kjær, and P. Christensen, "Modelling and simulation of VSC-HVDC connection for wind power plants," in *Proceeding of the 5th Nordic Wind Power Conference*, 2009.

[22] M. Ucar, Ş. ÖZDEMİR, and E. ÖZDEMİR, "A unified series-parallel active filter system for nonperiodic disturbances," *Turkish Journal of Electrical Engineering & Computer Sciences,* vol. 19, no. 4, pp. 575-596, 2011.

[23] Z. J. X. Z. C. Hairong, "Startup Procedures for the VSC-HVDC System [J]," *Transactions of China Electrotechnical Society,* vol. 9, 2009.

[24] M. Changizian and A. Shoulaie, "Research on Effective Parameters on Overvoltage and Inrush Current in Starting-up of VSC-HVDC System," in *2019 International Power System Conference (PSC)*, 9-11 Dec. 2019 2019, pp. 410-416, doi: 10.1109/PSC49016.2019.9081480.

[25] A.-I. Stan and D.-I. Stroe, "Control of VSC-based HVDC transmission system for offshore wind power plants," *Departament of Energy Tehnology Aalborg University, Denmark,* 2010.

[26] D. Nilsson, "DC distribution systems," Göteborg University, Department of Enargy and Environment, 2005.

[27] Y. Liang and C. Nwankpa, "A new type of STATCOM based on cascading voltage-source inverters with phase-shifted unipolar SPWM," *IEEE transactions on industry applications,* vol. 35, no. 5, pp. 1118-1123, 1999.

[28] N. R. Mahajan, "System protection for power electronic building block based DC distribution systems," 2004.